

Colestilan decreases weight gain by enhanced NEFA incorporation in biliary lipids and fecal lipid excretion

Kanami Sugimoto-Kawabata,¹ Hiroshi. Shimada,¹ Kaoru. Sakai,¹ Kazuo. Suzuki,¹

Thomas. Kelder,² Elsbet. J. Pieterman,² Louis. H. Cohen,² Louis. M. Havekes,²

Hans. M. Princen,² Anita. M. van den Hoek²

¹Metabolic Diseases, Department I, Pharmacology Research Laboratories 2,

Mitsubishi Tanabe Pharma Corporation,

2-2-50, Kawagishi, Toda-shi, Saitama 335-8505, Japan

²The Netherlands Organization for Applied Scientific Research- Metabolic Health Research,

Gaubius Laboratory, Zernikedreef 9, 2333 CK, Leiden, the Netherlands

Abbreviated title: BAS increases biliary lipid synthesis and fecal excretion

Corresponding author: Kanami Sugimoto-Kawabata

Metabolic Diseases, Department I, Pharmacology Research Laboratories 2,

Mitsubishi Tanabe Pharma Corporation,

2-2-50, Kawagishi, Toda-shi, Saitama 335-8505, Japan

TEL +81-48-433-8094, FAX +81-48-433-8161

E-mail: Sugimoto.Kanami@mk.mt-pharma.co.jp

Abbreviations

BAS	Bile acid sequestrant
CE	Cholesteryl esters
E3L	<i>APOE*3 Leiden</i>
FXR	Farnesoid X receptor
GLP-1	Glucagon-like peptide 1
GPBAR1	G-protein-coupled bile acid receptor
HGP	Hepatic glucose production
HPTLC	High-performance thin layer chromatography
LXR	Liver X receptor
RER	Respiratory exchange ratio
SHP	Small heterodimer partner
SE	Standard errors
TG	Triglyceride
TNO	The Netherlands Organization for Applied Scientific Research

ABSTRACT

Bile acid sequestrants (BASs) are cholesterol-lowering drugs that also affect hyperglycemia. The mechanism by which BASs exert these and other metabolic effects beyond cholesterol lowering remains poorly understood. The present study aimed to investigate the effects of a BAS, colestilan, on body weight, energy expenditure, and glucose and lipid metabolism and its mechanisms of action in high-fat-fed hyperlipidemic *APOE*3 Leiden* (E3L) transgenic mice. Mildly insulin resistant E3L mice were fed a high-fat diet with or without 1.5% colestilan for 8 weeks. Colestilan treatment decreased body weight, visceral and subcutaneous fat, and plasma cholesterol and triglyceride levels but increased food intake. Blood glucose and plasma insulin levels were decreased, and hyperinsulinemic-euglycemic clamp analysis demonstrated improved insulin sensitivity, particularly in peripheral tissues. In addition, colestilan decreased energy expenditure and physical activity, whereas it increased the respiratory exchange ratio, indicating that colestilan induced carbohydrate catabolism. Moreover, kinetic analysis revealed that colestilan increased [³H]-NEFA incorporation in biliary cholesterol and phospholipids and increased fecal lipid excretion. Gene expression analysis in liver, fat and muscle supported the above findings. In summary, colestilan decreases weight gain and improves peripheral insulin sensitivity in high-fat-fed E3L mice by enhanced NEFA incorporation in biliary lipids and increased fecal lipid excretion.

Supplementary key words: adipose tissue, bile acid sequestrant, colestilan, hyperinsulinemic–euglycemic clamp, insulin sensitivity, NEFA incorporation

Introduction

Bile acid sequestrants (BASs) have been used for many years as an effective therapy for dyslipidemia. The cholesterol-lowering properties of BASs entail the binding of bile acids in the intestine, thereby reducing the enterohepatic circulation of bile acids and leading to an accelerated conversion of cholesterol to bile acids (1). More recently, BASs have been shown to improve hyperglycemia in diabetic animals and in patients with type 2 diabetes (2-11). In addition, the effects of bile acids and BASs on energy expenditure have been reported in animal studies (12, 13). Although various mechanisms of action regarding BAS have been proposed, including the farnesoid X receptor (FXR)–small heterodimer partner (SHP)–liver X receptor (LXR) pathway and involvement of a G-protein-coupled bile acid receptor (GPBAR1; TGR5), and glucagon-like peptide 1 (GLP-1) (4, 12, 14-17), the exact mechanisms by which BASs exert their metabolic effects beyond cholesterol lowering remain unclear.

Colestilan/colestimide/MCI-196, a BAS, has been reported to significantly decrease body weight, body mass index, and visceral fat in obese patients with hypercholesterolemia after 24 weeks of treatment (5). Furthermore, colestilan decreases blood glucose and HbA_{1c} levels in Japanese patients with type 2 diabetes (18). To further evaluate the effects of colestilan on weight gain, energy expenditure, and glucose and lipid metabolism and to determine its

underlying mechanism of action, we investigated the effects of colestilan using high-fat-fed *APOE*3 Leiden* (E3L) transgenic mice. We used E3L mice because their lipoprotein profile closely resembles that of humans (19) and they are responsive to all lipid-lowering drugs presently used in clinical practice (20, 21). When fed a high-fat diet, these mice become mildly insulin resistant (22, 23). We hypothesized that colestilan induces hepatic cholesterol/bile acid/phospholipid synthesis, leading to increased glycerol/NEFA incorporation in biliary lipids. The increased glycerol/NEFA incorporation, derived from triglyceride (TG) lipolysis in adipose tissue, together with increased fecal lipid excretion would thereby contribute to decreased body weight and improved insulin sensitivity.

To investigate our hypothesis, we used infusion of radiolabeled glycerol and NEFA and determined their subsequent conversions to biliary lipids. In addition, we evaluated the effects of colestilan on fecal excretion, energy metabolism, insulin sensitivity and analysis of gene expression relevant to lipid and glucose metabolism in liver, adipose tissue and muscle.

Methods

Experimental animals

Heterozygous E3L transgenic male mice aged 10–14 weeks were established at The Netherlands Organization for Applied Scientific Research (TNO) animal facility. They were housed in a temperature-controlled room on a 12-h light–dark cycle with water and food *ad*

libitum. Animal experiments were performed according to EU regulation 86/609/EC, CoE ETS 123 and the Dutch Experiments on Animals Act, which includes approval by the Institutional Animal Care and Use Committee of TNO. Several of the measurements and results described here were repeated in either another cohort of APOE*3Leiden mice (plasma parameters, feces composition, hyperinsulinemic-euglycemic clamp experiments and metabolic cage experiments) or in another diabetic mouse model KKA^y mice (plasma parameters, feces composition and the results of the hyperinsulinemic-euglycemic clamp experiments). Data acquired were in line with data presented herein.

Diets

After a run-in period on a high-fat diet (47 kCal% beef tallow, 20 kCal% protein, 33 kCal% carbohydrates; Hope Farms, Woerden, the Netherlands) for 10–12 weeks, E3L mice were divided on the basis of body weight, blood glucose, plasma cholesterol, and plasma insulin (all measured after 4-h fasting) into 2 groups (week 0). The control group was fed a high-fat diet, whereas the colestilan group was fed a high-fat diet containing 1.5% (w/w) colestilan (Mitsubishi Tanabe Pharma Corporation, Tokyo, Japan). The colestilan was added to the diet, leading to a slightly lower caloric density of the diet (4.48 vs. 4.55 kCal/g). Body weight and food intake were monitored every week.

Analysis of plasma parameters

Blood samples were collected by tail bleeding after 4-h fasting, except for clamp and flux analyses, where the animals were fasted overnight. Blood glucose levels were measured using the “Freestyle blood glucose measurement system” from Disetronic Medical Systems BV (Vianen, the Netherlands) according to the manufacturer’s instructions. Plasma total cholesterol and TG levels were measured using the assay reagents from Roche Diagnostics (Almere, the Netherlands). Plasma insulin levels were measured using a kit from Linco Research (St. Charles, MO, USA). Plasma NEFA was measured using the NEFA C kit from WAKO (Neuss, Germany).

Fecal lipid analysis

At weeks 7 and 8 of the study period, feces were collected from 3 subgroups per treatment group during 3 different periods of 3–4 days (9 samples/group), and neutral sterol and bile acid contents were analyzed by gas chromatography as described previously (24).

[¹⁴C]-glycerol/[³H]-NEFA infusion and bile analysis

At weeks 9 and 10, [¹⁴C]-glycerol/[³H]-NEFA infusion and bile cannulation were performed by procedures similar to those described previously (25, 26). After overnight fasting, the mice were anesthetized [12.5 mg/kg midazolam (Gentheron, Nijmegen, the Netherlands), 25 mg/kg fluanisone (Janssen Pharmaceutica, Beerse, Belgium), 0.79 mg/kg fentanyl citrate (Janssen Pharmaceutica)]. The gall bladder was cannulated, and an infusion needle was injected into the inferior vena cava. [³H]-oleate and [¹⁴C]-glycerol were

continuously infused beginning at $t = 0$ min, and bile was collected at 30-min intervals until $t = 180$ min. Simultaneously, a blood sample was collected from the tip of the tail. After 180 min, the mice were sacrificed and abdominal (epididymal) fat, subcutaneous fat, muscle (femoralis), and the liver were harvested. NEFA/glycerol concentrations were determined from plasma samples. Free glycerol concentrations were measured using a free glycerol kit (Sigma, St. Louis, MO, USA). Bile flow, [^3H]-bile acid and total bile acid flow, [^3H]-cholesterol and total cholesterol flow, and [^3H]-phospholipid and total phospholipid flow were determined in the collected bile. Bile acid concentrations were measured using a bile acid kit (Lucron Bioproducts, Milsbeek, the Netherlands). Bile acids were isolated using Sep-Pak C18 cartridges. Subsequently, ^3H -dpm incorporation in bile acids was determined. Cholesterol was extracted from bile (Bligh and Dyer method), isolated from other lipids, and quantified by high-performance thin layer chromatography (HPTLC); [^3H]-cholesterol was determined by counting ^3H -dpm in scraped HPTLC bands. Phospholipids were determined using the Phospholipids B kit (WAKO). [^3H]-phospholipids were determined by counting ^3H -dpm in scraped HPTLC bands. Levels of ^{14}C incorporation in bile acids, cholesterol, and phospholipids were too low to be measured, making it impossible to determine the conversion of glycerol to biliary lipids.

Fat weight and hepatic lipid content

After glycerol/NEFA infusion, abdominal (epididymal) fat, subcutaneous fat, liver, and femoral muscle tissue were harvested and weighed. The hepatic lipid content [free cholesterol, TG, and cholesteryl esters (CE)] was determined by procedures described previously (27). In brief, 10–20 mg of tissue was homogenized in PBS, the protein content was measured, and lipids were extracted and separated by HPTLC on silica gel plates. Lipid spots were stained with a coloring reagent (5 g $\text{MnCl}_2 \cdot 4\text{H}_2\text{O}$, 32 ml 95%–97% H_2SO_4 added to 960 ml $\text{CH}_3\text{OH}:\text{H}_2\text{O}$ 1:1 v/v) and quantified using TINA[®] version 2.09 software (Raytest, Straubenhardt, Germany).

Hyperinsulinemic–euglycemic clamp analysis

Different groups of mice were used for these experiments. Hyperinsulinemic–euglycemic clamp analysis was performed at week 9 as described previously (28). In brief, after overnight fasting, the mice were anesthetized [0.5 ml/kg Hypnorm (Janssen Pharmaceutica), 12.5 mg/g midazolam (Gentho)]. An infusion needle was inserted into one of the tail veins, and basal glucose parameters were determined by infusing D-[³H]-glucose. Thereafter, the mice were given a bolus of insulin; a hyperinsulinemic clamp was initiated by continuously infusing insulin and D-[³H]-glucose. Blood samples (<3 μl) were collected at 10-min intervals (tail bleeding) to monitor blood glucose levels. A variable infusion of 12.5% D-glucose solution (in PBS) was initiated at time 0 and adjusted to maintain blood glucose at approximately 7.0 mmol/l. When steady-state glucose levels were reached (approximately 1 h

after initiating the insulin infusion), blood samples were collected at 20-min intervals for 1 h to determine insulin-stimulated glucose turnover.

Measurements in metabolic cages

Different groups of mice were used for this experiment. The mice were individually housed in metabolic cages (Columbus Instruments, Columbus, OH, USA) and fed a powdered diet *ad libitum*. Metabolic parameters in the mice were assessed at weeks 1 and 3 for 2–3 days in metabolic cages (after 1-day acclimatization in the same cage) (29). The following variables were continuously monitored: total food intake, total physical activity, total O₂ consumption (expressed as VO₂ ml kg⁻¹ h⁻¹), and total CO₂ production (VCO₂ ml kg⁻¹ h⁻¹). The respiratory exchange ratio (RER) and energy expenditure (kcal kg⁻¹ h⁻¹) were determined from these variables.

Gene expression analysis

Different groups of mice were used for this experiment. After 8 weeks of colestilan treatment, livers, (perigonadal) adipose tissues and muscles were removed after 4-h fasting and frozen in liquid N₂ for microarray analysis. RNA was extracted using RNeasy kit (Qiagen, Venlo, The Netherlands), purified using the RNeasy kit (Qiagen, Venlo, The Netherlands), and analyzed for its integrity on Aligent chips (“lab on chip” RNA 6000 Nano assay). If not sufficiently intact, RNA was extracted again. For both groups, equal quantities of individual RNA samples were pooled and labeled in duplicate (biotin-labeled cRNA

synthesis) for hybridization. Each sample was hybridized with Affymetrix mouse array MOE430A (containing probes for 22625 genes) in duplicate. The hybridization signals were analyzed using Affymetrix software and stored in primary data files. Preprocessing and quality control of the microarray data was performed using the ArrayAnalysis.org pipeline (<http://www.arrayanalysis.org>). All samples passed the QC. Raw signal intensities were normalized using the GCRMA algorithm applied across all arrays in the dataset. Probe-level signals were summarized to gene-level intensities using the custom MNBI CDF-file (Entrez Gene annotation, version 16.0.0). This resulted in expression values for 12251 genes, represented by unique Entrez Gene identifiers. Normalized intensities were log transformed (base2) and fold changes were calculated based on the averages of the two technical replicates within each group.

Statistical analysis

All data are expressed as means \pm standard errors (SE). The significance of differences was calculated using Student's *t*-test. *p* values <0.05 were considered statistically significant.

Results

Colestilan decreases body weight, fat mass, and plasma lipids despite higher caloric intake

To induce mild obesity and insulin resistance, male E3L mice were fed a high-fat diet for 10 weeks. Thereafter, the same diet with or without colestilan was administered for 8 weeks. Body weight in the colestilan group was significantly decreased compared with that in the control group from week 2 of treatment (Fig. 1A). The colestilan group exhibited significantly increased food intake from week 1 or 2 (Fig. 1B), resulting in an on average 7.5-15% higher caloric intake and indicating that the decrease in body weight following colestilan treatment was not due to decreased food intake. Quantitative analysis of adipose tissue deposits at the end of the study revealed that colestilan treatment significantly decreased abdominal (epididymal) and subcutaneous fat (Fig. 1C). The liver and (femoral) muscle tissue weights did not differ between the groups (Fig. 1C), indicating that the decrease in body weight was primarily caused by a substantial decrease in abdominal and subcutaneous fat.

Plasma cholesterol levels in the control group remained stable during the study period (approximately 7 mmol/l) (Fig. 1D). As expected for BAS, colestilan significantly decreased plasma cholesterol levels at weeks 4 and 8 (Fig. 1D) and resulted in significantly decreased plasma TG levels at weeks 4 and 8 (Fig. 1E).

These results indicate that colestilan treatment decreases body weight and fat mass of mice despite increased caloric intake.

Colestilan decreases blood glucose and plasma insulin levels by improving peripheral insulin resistance

Because it was recently reported that colestilan improves glycemic control (in addition to its effects on plasma LDL cholesterol) in type 2 diabetic patients (5, 18), we next measured blood glucose and plasma insulin levels in E3L mice. Control E3L mice exhibited mild hyperglycemia, which was significantly attenuated after colestilan treatment for 4–8 weeks (Fig. 2A). Plasma insulin levels in the colestilan group were significantly decreased compared with the levels in the control group at weeks 4 and 8 (Fig. 2B), indicating that colestilan improved insulin sensitivity. To further confirm the effect of colestilan on insulin sensitivity, we performed hyperinsulinemic–euglycemic clamp analysis after overnight fasting. Whole-body glucose disposal (i.e., the glucose infusion rate) in the colestilan group was significantly higher than that in control group (Fig. 2C). Under hyperinsulinemic conditions, whole-body glucose uptake in the colestilan group was significantly increased compared with that in the control group (Fig. 2D). The difference in hepatic glucose production (HGP) under basal and hyperinsulinemic conditions was expressed as the percentage of basal HGP to obtain the hepatic insulin sensitivity index. Colestilan treatment did not alter the hepatic insulin sensitivity index (Fig. 2E), indicating that the drug improved

peripheral insulin resistance without affecting hepatic insulin sensitivity.

Collectively, these observations and the decrease in adipose tissue (Fig. 1C) support the contention that the colestilan-treated mice become more insulin sensitive.

Colestilan decreases energy expenditure and induces carbohydrate catabolism

The decreased body weight and increased food intake in the colestilan group suggest that colestilan increases energy expenditure. However, the current literature pertaining to this issue suggests that BASs treatment would actually result in decreased energy expenditure (12, 17). No direct experimental studies to address this issue have been performed to date. To clarify this issue, we measured O₂ consumption, CO₂ production, food intake, and physical activity using metabolic cage analysis. We calculated RER, which gives information on the substrate used for energy generation, from the ratio of O₂ consumption to CO₂ production. Moreover, we calculated O₂ consumption-related energy expenditure.

Metabolic cage analysis with continuous measurements of food consumption during a period of 2–3 days confirmed that colestilan increased food intake (data not shown). At week 1, physical activity of the mice was the same during the daytime, i.e., sleeping time; however, the colestilan-treated mice exhibited significantly lower activity during the night (Fig. 3A). Furthermore, O₂-consumption-related energy expenditure of the colestilan-treated mice was significantly lower than that of the control group (Fig. 3B), conceivably caused by lower physical activity of the mice. The decrease in physical activity and energy expenditure was

also observed at week 3 (data not shown). RER was significantly higher in the colestilan group during the night of day 6 (Fig. 3C); this difference became more pronounced after 3 weeks of treatment. At days 19 and 20, the mean RER of the colestilan group was significantly increased at the end of the light period and at the beginning of the dark period (Fig. 3D).

These results reveal that the colestilan-treated mice use relatively more carbohydrates than fatty acids for energy generation, which constitutes an additional explanation for the increased glucose uptake in peripheral tissues, as observed in clamp analysis.

Colestilan increases fecal lipid excretion without changing fatty acid balance

Because the decreased body weight and increased food intake could not be explained by increased energy expenditure, we also analyzed fecal excretion of fatty acids, bile acids, and neutral sterols. We hypothesized that the decrease in plasma lipids could be attributed to an increased flow of biliary lipids from the liver to the feces. First, we measured liver weight and hepatic lipid contents, which did not change significantly, except for the free cholesterol level, which was slightly but significantly increased (Fig. 4A).

Subsequently, we analyzed fecal lipids and found more than 7- and 3-fold increases in bile acid and neutral sterol excretion, respectively (Fig. 4B). Moreover, the colestilan group displayed significantly increased total fecal fatty acid excretion than the control group (Fig. 4C). Because the colestilan-treated mice had higher food intake (Fig. 1B), the fatty acid

balance was calculated from the difference in the total fatty acid intake and total fatty acids excreted in the feces. The fatty acid balance in these mice remained constant compared with that in control group (Fig. 4D), indicating that the same amount of fat was absorbed in the control and colestilan-treated animals.

Colestilan increases the conversion of NEFA to biliary lipids

The observations of lower energy expenditure and unaltered fat absorption do not provide an explanation for the decrease in weight gain, in particular in adipose tissue, during colestilan treatment. Therefore, we tested the hypothesis that colestilan increased NEFA incorporation in biliary lipids by measuring the flow of [³H]-radiolabeled plasma fatty acids into bile during bile duct cannulation and by determining the mass and incorporation of [³H]-NEFA-derived radioactivity in biliary bile acids, cholesterol, and phospholipids. Compared with the control group, colestilan treatment tended ($p = 0.08$) to induce higher bile production over 180 min (Fig. 5G). Total [³H]-NEFA-derived radioactivity in cholesterol (Fig. 5C) and phospholipids (Fig. 5E) in bile were both significantly increased in the colestilan group. [³H]-NEFA-derived radioactivity in bile acids increased in the colestilan group; however, this increase was not significant ($p = 0.14$) (Fig. 5A). In contrast, compared with the control group, the colestilan-treated group exhibited no difference in non-labeled bile acids (Fig. 5B), cholesterol (Fig. 5D), and phospholipids (Fig. 5F) in bile.

These observations indicate that colestilan increases biliary lipid synthesis using fatty

acids as a substrate in the liver. Consistent with the increased use of NEFA by the liver for conversion to biliary lipids, plasma NEFA levels in the colestilan group were decreased during treatment (Fig. 5H).

Colestilan affects expression of genes involved in lipid and glucose metabolism.

To further investigate the mechanism by which colestilan affects metabolism, we determined the expression profile of 12251 well-characterized mouse genes in liver, adipose tissue and muscle. A selection of genes involved in lipid and glucose metabolism is depicted as Supplemental figure. From this selection, only those genes that were significantly affected by colestilan treatment in either one or more tissues are depicted in Figure 6. The hepatic gene expression patterns were mostly directed and related to activation of fatty acids (*Acs15* and *Acss2*), formation of phospholipids (*Pcyt1a*, *Cds2* and *Lpcat3*) and strong enhancement of the flux from intermediary metabolites, starting from acetyl-CoA to cholesterol and bile acids, in line with the enhanced synthesis of phospholipids, cholesterol and bile acids. The latter was reflected by the clear increase of genes involved in cholesterol (*Acly*, *Acat2*, *Hmgcr*, *Fdft1*) and bile acid synthesis (*Cyp7a1*) together with a decrease in expression of *Nr0B2* (SHP) as major suppressor of *Cyp7a1* expression. Although hepatic *Ppara* gene expression was strongly upregulated, this was not accompanied by stimulation of other genes involved in fatty acid activation and oxidation, most likely explained by the fact that the mRNAs were isolated after 4h fasting whereas PPAR- α is activated under nutrient-deficient conditions as

an adaptive response to prolonged fasting. In contrast, the NEFA incorporation study was performed after overnight fasting, a condition known to activate fatty acid oxidation.

In adipose tissue upregulation of the expression of several genes involved in fatty acid transport (*Fabp1*, *Fabp6* and *Slc27a2*) was observed, but also an enhanced expression of *Slc2a4*, the gene encoding for GLUT4, the most important protein for insulin-regulated glucose uptake. In contrast, in muscle the expression of *Slc2a4* was decreased, suggesting that the improvement of peripheral insulin sensitivity by colestilan is due to increased glucose uptake in adipose tissue.

In general, genes involved in insulin signaling were found to be relatively unaffected. This does however not mean that colestilan did not have an effect, since regulation of the insulin signaling pathway is primarily determined by the phosphorylation state of the proteins therein.

Discussion

In this paper, we demonstrated that the treatment of dyslipidemic and mildly obese and insulin-resistant E3L mice with colestilan markedly improved body weight, hyperglycemia, and dyslipidemia. Of note, colestilan decreased the amount of abdominal and subcutaneous adipose tissue and improved peripheral insulin sensitivity. Mechanistic studies revealed that the drug increased the synthesis of biliary lipids using fatty acids as a substrate in the liver.

Surprisingly, the phenotypic changes in body weight and fat deposition were accompanied by increased food intake, indicating that decreases in body weight and blood glucose levels did not result from decreased food intake. This decrease in body weight was not specific for E3L mice because colestilan treatment exerted a similar effect in another mouse model for obesity and insulin resistance, KKA^y mice (unpublished observation). Although their food intake was increased, the fatty acid balance in the colestilan-treated E3L mice remained the same as that in the control mice because colestilan profoundly increased fecal fatty acid excretion.

Colestilan improved glycemic control in the high-fat-fed E3L mice, as reflected by significant reductions in blood glucose and plasma insulin levels, in line with decreased glucose and HbA1c levels (beside LDL cholesterol) observed in type 2 diabetic patients with or without hypercholesterolemia (2-5, 18, 30, 31). Hyperinsulinemic–euglycemic clamp analysis demonstrated that colestilan improved insulin sensitivity in the peripheral tissues without affecting the liver. Consistent with this finding, the amount of visceral and subcutaneous adipose tissues was decreased, whereas liver weight and the hepatic TG content remained unchanged, the latter in accordance with the inverse correlation between hepatic TG levels and insulin sensitivity as reported previously (32).

Multiple mechanisms have been proposed to explain the anti-diabetic effects of BASs in the literature on the basis of the existing knowledge of bile acid biology (7, 11, 17). Cholestyramine has been recently reported to improve glycemic control in Zucker diabetic

fatty rats by enhancing incretin responses such as GLP-1 and peptide YY, for which the FXR–SHP–LXR pathway was not required (14). Another study in diet-induced obese rats demonstrated that colestevlam treatment decreased plasma glucose levels by improving insulin resistance secondary to inducing GLP-1 secretion (15). In a clinical study, colestilan decreased postprandial plasma glucose concentrations and increased GLP-1 levels in patients with type 2 diabetes (4). Because we did not measure GLP-1 levels, we cannot exclude the possibility that increased GLP-1 secretion contributes to the reduction in body weight and improved metabolic control in the colestilan-treated E3L mice.

Interestingly, the beneficial effects of colestilan on obesity and insulin sensitivity were not caused by an increase in energy expenditure. In fact, energy expenditure was found to be decreased. Simultaneously, the calculated RER in the colestilan-treated mice was significantly increased, indicating an enhanced preference for carbohydrates over fats for energy production. Remarkably, this elevated glucose catabolism occurs even under the consumption of a high-fat diet. The latter data together with improved peripheral insulin sensitivity provide an explanation for the increased whole-body glucose uptake in the colestilan-treated mice. Transcriptome analysis confirmed these data showing that the gene encoding the glucose transporter GLUT4 was upregulated in adipose tissue and not in muscle, suggesting increased glucose uptake in fat.

In line with our findings, it has been reported that bile acids promote energy expenditure

by TGR5 activation (12) and that a lowered bile acid pool size reduces energy expenditure (16). This led to the suggestion that BAS treatment would result in decreased energy expenditure (17). However, in humans, BAS treatment had no effect on energy expenditure and no correlation with plasma bile acid levels was found (33). In the present study, the decrease in energy expenditure is possibly related to the observed decrease in physical activity.

We have demonstrated for the first time to our knowledge that BAS increases NEFA incorporation in biliary lipids. The results of [³H]-NEFA infusion experiments strongly support our working hypothesis: [³H]-NEFA-derived radioactivity in biliary cholesterol and phospholipids in the colestilan group was significantly higher than that in the control group, whereas incorporation in biliary bile acids tended to be increased, indicating enhanced hepatic synthesis of biliary lipids using fatty acids as a substrate. Gene expression profiling in the liver supported this mechanism by demonstrating upregulation of genes involved in activation of fatty acids (*Acs15* and *Acss2*), formation of phospholipids (*Pcyt1a*, *Cds2* and *Lpcat3*) and synthesis of cholesterol (*Acly*, *Acat2*, *Hmgcr*, *Fdft1*) and bile acids (*Cyp7a1*). Furthermore, these results combined with the observed decreases in adipose tissue deposits and plasma NEFA levels support the contention of colestilan-induced enhanced TG efflux from adipose tissue. Decreased plasma NEFA levels induced by colestilan treatment may constrain the energy metabolism toward higher catabolism of carbohydrates, as reflected by

the elevated RER values. In concert with the decreased visceral obesity, this may contribute to increased insulin sensitivity.

In conclusion, we demonstrated that colestilan decreased weight gain and improved peripheral insulin sensitivity in high-fat-fed male E3L mice by enhanced NEFA incorporation in biliary lipids and increased fecal lipid excretion. Our results provide a potential mechanistic basis for the effects of BASs in humans.

Acknowledgments

The authors thank Dr. Peter Voshol for assistance with hyperinsulinemic–euglycemic clamp analysis and [^{14}C]-glycerol/[^3H]-NEFA infusion analysis and discussions, Dr. Sjoerd van den Berg for assistance with metabolic cage analysis, and Dr. Kenji Arakawa and Dr. Shinichi Ishii for the discussion. All authors were involved in designing the studies described in this paper and have approved this final version.

REFERENCES

1. Princen, H. M., S. Post, and J. Twisk. 1997. Regulation of bile acid biosynthesis. *Curr Pharm Design* **3**: 59-84.
2. Suzuki, T., K. Oba, S. Futami, K. Suzuki, M. Ouchi, Y. Igari, N. Matsumura, K. Watanabe, Y. Kigawa, and H. Nakano. 2006. Blood glucose-lowering activity of colestimide in patients with type 2 diabetes and hypercholesterolemia: a case-control study comparing colestimide with acarbose. *J Nippon Med Sch* **73**: 277-284.
3. Yamakawa, T., T. Takano, H. Utsunomiya, K. Kadonosono, and A. Okamura. 2007. Effect of colestimide therapy for glycemic control in type 2 diabetes mellitus with hypercholesterolemia. *Endocr J* **54**: 53-58.
4. Suzuki, T., K. Oba, Y. Igari, N. Matsumura, K. Watanabe, S. Futami-Suda, H. Yasuoka, M. Ouchi, K. Suzuki, Y. Kigawa, and H. Nakano. 2007. Colestimide lowers plasma glucose levels and increases plasma glucagon-like PEPTIDE-1 (7-36) levels in patients with type 2 diabetes mellitus complicated by hypercholesterolemia. *J Nippon Med Sch* **74**: 338-343.
5. Suzuki, T., K. Oba, S. Futami-Suda, K. Suzuki, M. Ouchi, Y. Igari, N. Matsumura, K. Watanabe, Y. Kigawa, and H. Nakano. 2007. Effects of colestimide on blood glucose-lowering activity and body weight in patients with type 2 diabetes and hypercholesterolemia. *J Nippon Med Sch* **74**: 81-84.

6. Bays, H. E., and R. B. Goldberg. 2007. The 'forgotten' bile acid sequestrants: is now a good time to remember? *Am J Ther* **14**: 567-580.
7. Staels, B., and F. Kuipers. 2007. Bile acid sequestrants and the treatment of type 2 diabetes mellitus. *Drugs* **67**: 1383-1392.
8. Bays, H. E., R. B. Goldberg, K. E. Truitt, and M. R. Jones. 2008. Colesevelam hydrochloride therapy in patients with type 2 diabetes mellitus treated with metformin: glucose and lipid effects. *Arch Intern Med* **168**: 1975-1983.
9. Fonseca, V. A., J. Rosenstock, A. C. Wang, K. E. Truitt, and M. R. Jones. 2008. Colesevelam HCl improves glycemic control and reduces LDL cholesterol in patients with inadequately controlled type 2 diabetes on sulfonylurea-based therapy. *Diabetes Care* **31**: 1479-1484.
10. Goldberg, R. B., V. A. Fonseca, K. E. Truitt, and M. R. Jones. 2008. Efficacy and safety of colesevelam in patients with type 2 diabetes mellitus and inadequate glycemic control receiving insulin-based therapy. *Arch Intern Med* **168**: 1531-1540.
11. Goldfine, A. B. 2008. Modulating LDL cholesterol and glucose in patients with type 2 diabetes mellitus: targeting the bile acid pathway. *Curr Opin Cardiol* **23**: 502-511.
12. Watanabe, M., S. M. Houten, C. Mataka, M. A. Christoffolete, B. W. Kim, H. Sato, N. Messaddeq, J. W. Harney, O. Ezaki, T. Kodama, K. Schoonjans, A. C. Bianco, and J.

Auwerx. 2006. Bile acids induce energy expenditure by promoting intracellular thyroid hormone activation. *Nature* **439**: 484-489.

13. Mabayo, R. T., M. Furuse, A. Murai, and J. Okumura. 1995. Cholestyramine alters the lipid and energy metabolism of chicks fed dietary medium- or long-chain triacylglycerol. *Lipids* **30**: 839-845.

14. Chen, L., J. McNulty, D. Anderson, Y. Liu, C. Nystrom, S. Bullard, J. Collins, A. L. Handlon, R. Klein, A. Grimes, D. Murray, R. Brown, D. Krull, B. Benson, E. Kleymenova, K. Remlinger, A. Young, and X. Yao. 2010. Cholestyramine reverses hyperglycemia and enhances glucose-stimulated glucagon-like peptide 1 release in Zucker diabetic fatty rats. *J Pharmacol Exp Ther* **334**: 164-170.

15. Shang, Q., M. Saumoy, J. J. Holst, G. Salen, and G. Xu. 2010. Colesevelam improves insulin resistance in a diet-induced obesity (F-DIO) rat model by increasing the release of GLP-1. *Am J Physiol Gastrointest Liver Physiol* **298**: G419-424.

16. Watanabe, M., Y. Horai, S. M. Houten, K. Morimoto, T. Sugizaki, E. Arita, C. Mataka, H. Sato, Y. Tanigawara, K. Schoonjans, H. Itoh, and J. Auwerx. 2011. Lowering bile acid pool size with a synthetic farnesoid X receptor (FXR) agonist induces obesity and diabetes through reduced energy expenditure. *J Biol Chem* **286**: 26913-26920.

17. Out, C., A. K. Groen, and G. Brufau. 2012. Bile acid sequestrants: more than simple resins. *Curr Opin Lipidol* **23**: 43-55.

18. Kondo, K., and T. Kadowaki. 2010. Colestilan monotherapy significantly improves glycaemic control and LDL cholesterol levels in patients with type 2 diabetes: a randomized double-blind placebo-controlled study. *Diabetes Obes Metab* **12**: 246-251.
19. van Vlijmen, B. J., A. M. van den Maagdenberg, M. J. Gijbels, H. van der Boom, H. HogenEsch, R. R. Frants, M. H. Hofker, and L. M. Havekes. 1994. Diet-induced hyperlipoproteinemia and atherosclerosis in apolipoprotein E3-Leiden transgenic mice. *J Clin Invest* **93**: 1403-1410.
20. Krause, B. R., and H. M. Princen. 1998. Lack of predictability of classical animal models for hypolipidemic activity: a good time for mice? *Atherosclerosis* **140**: 15-24.
21. Zadelaar, S., R. Kleemann, L. Verschuren, J. de Vries-Van der Weij, J. van der Hoorn, H. M. Princen, and T. Kooistra. 2007. Mouse models for atherosclerosis and pharmaceutical modifiers. *Arterioscler Thromb Vasc Biol* **27**: 1706-1721.
22. Muurling, M., R. P. Mensink, H. Pijl, J. A. Romijn, L. M. Havekes, and P. J. Voshol. 2003. A fish oil diet does not reverse insulin resistance despite decreased adipose tissue TNF-alpha protein concentration in ApoE-3*Leiden mice. *J Nutr* **133**: 3350-3355.
23. Kleemann, R., M. van Erk, L. Verschuren, A. M. van den Hoek, M. Koek, P. Y. Wielinga, A. Jie, L. Pellis, I. Bobeldijk-Pastorova, T. Kelder, K. Toet, S. Wopereis, N. Cnubben, C. Evelo, B. van Ommen, and T. Kooistra. 2010. Time-resolved and tissue-specific systems analysis of the pathogenesis of insulin resistance. *PLoS One* **5**: e8817.

24. Post, S. M., R. de Crom, R. van Haperen, A. van Tol, and H. M. Princen. 2003. Increased fecal bile acid excretion in transgenic mice with elevated expression of human phospholipid transfer protein. *Arterioscler Thromb Vasc Biol* **23**: 892-897.
25. Teusink, B., P. J. Voshol, V. E. Dahlmans, P. C. Rensen, H. Pijl, J. A. Romijn, and L. M. Havekes. 2003. Contribution of fatty acids released from lipolysis of plasma triglycerides to total plasma fatty acid flux and tissue-specific fatty acid uptake. *Diabetes* **52**: 614-620.
26. Voshol, P. J., N. R. Koopen, J. M. de Vree, R. Havinga, H. M. Princen, R. P. Elferink, A. K. Groen, and F. Kuipers. 2001. Dietary cholesterol does not normalize low plasma cholesterol levels but induces hyperbilirubinemia and hypercholanemia in Mdr2 P-glycoprotein-deficient mice. *J Hepatol* **34**: 202-209.
27. Havekes, L. M., E. C. de Wit, and H. M. Princen. 1987. Cellular free cholesterol in Hep G2 cells is only partially available for down-regulation of low-density-lipoprotein receptor activity. *Biochem J* **247**: 739-746.
28. van den Hoek, A. M., P. J. Voshol, B. N. Karnekamp, R. M. Buijs, J. A. Romijn, L. M. Havekes, and H. Pijl. 2004. Intracerebroventricular neuropeptide Y infusion precludes inhibition of glucose and VLDL production by insulin. *Diabetes* **53**: 2529-2534.
29. van den Hoek, A. M., A. C. Heijboer, P. J. Voshol, L. M. Havekes, J. A. Romijn, E. P. Corssmit, and H. Pijl. 2007. Chronic PYY3-36 treatment promotes fat oxidation and

ameliorates insulin resistance in C57BL6 mice. *Am J Physiol Endocrinol Metab* **292**: E238-245.

30. Yamakawa, T., T. Kaneko, E. Shigematu, J. Kawaguchi, K. Kadonosono, S. Morita, and Y. Terauchi. 2011. Glucose-lowering effect of colestimide is associated with baseline HbA1c in type 2 diabetic patients with hypercholesterolemia. *Endocr J* **58**: 185-191.

31. Suzuki, T., K. Oba, Y. Igari, K. Watanabe, N. Matsumura, S. Futami-Suda, M. Ouchi, K. Suzuki, K. Sekimizu, Y. Kigawa, and H. Nakano. 2012. Effects of bile-acid-binding resin (colestimide) on blood glucose and visceral fat in Japanese patients with type 2 diabetes mellitus and hypercholesterolemia: an open-label, randomized, case-control, crossover study. *J Diabetes Complications* **26**: 34-39.

32. Voshol, P. J., P. C. Rensen, K. W. van Dijk, J. A. Romijn, and L. M. Havekes. 2009. Effect of plasma triglyceride metabolism on lipid storage in adipose tissue: studies using genetically engineered mouse models. *Biochim Biophys Acta* **1791**: 479-485.

33. Brufau, G., M. J. Bahr, B. Staels, T. Claudel, J. Ockenga, K. H. Boker, E. J. Murphy, K. Prado, F. Stellaard, M. P. Manns, F. Kuipers, and U. J. Tietge. 2010. Plasma bile acids are not associated with energy metabolism in humans. *Nutr Metab (Lond)* **7**: 73.

Figure Legends

Figure 1

Colestilan decreases body weight, fat mass, and plasma lipid levels and increases food intake.

*APOE*3 Leiden* (E3L) mice in the control and colestilan groups were given a high-fat diet and high-fat diet with 1.5% colestilan, respectively, for 8 weeks. Body weight (A) and food intake (B) were measured every week, and plasma cholesterol (D) and triglyceride (E) levels were measured after weeks 4 and 8 of colestilan treatment (n=20–21). Plasma was obtained from E3L mice that were fasted for 4 h. (C) Abdominal and subcutaneous fat, liver, and femoral muscle were removed and weighed after weeks 9 or 10 of colestilan treatment (n=11–12). Data are expressed as means \pm SE. $**p < 0.01$ vs. control by Student's *t*-test.

Figure 2

Colestilan decreases blood glucose and plasma insulin levels and improves whole-body and peripheral insulin sensitivity. Blood glucose (A) and plasma insulin (B) were measured after a 4-h fasting period in high-fat-fed E3L mice. At week 9, the glucose infusion rate (A), body glucose uptake under the hyperinsulinemic condition (B), and hepatic insulin sensitivity index (C) were determined by hyperinsulinemic–euglycemic clamp analysis after overnight fasting. Data are expressed as means \pm SE [n =20–21 (A, B), n=4–6 (C, D, E)]. $*p < 0.05$, $**p < 0.01$ vs. control by Student's *t*-test.

Figure 3

Colestilan decreases energy expenditure and induces carbohydrate catabolism. High-fat-fed E3L mice were placed in metabolic cages and analyzed at weeks 1 and 3 for 2–3 days. Food intake, physical activity (A), O₂ consumption, and CO₂ production were measured. Energy expenditure was calculated from O₂ consumption at week 1 (B). Respiratory exchange ratio (RER) was calculated from O₂ consumption and CO₂ production at week 1 (C) and week 3 (D). Data are expressed as means ± SE (n = 7–8). **p* < 0.05, ***p* < 0.01 vs. control by Student's *t*-test.

Figure 4

Colestilan increases fecal lipid excretion without changing the fatty acid balance. Feces were collected during weeks 7–8, and fecal bile acids (A), neutral sterols (A), and fatty acids (B) were measured after lipid extraction (n=9). Fatty acid balance was calculated from the difference between the total fatty acid intake and total fatty acid excreted in the feces (C). Hepatic lipids were measured after weeks 9 to 10 of colestilan treatment (n = 11–12) (D). Data are expressed as means ± SE. **p* < 0.05, ***p* < 0.01 vs. control by Student's *t*-test.

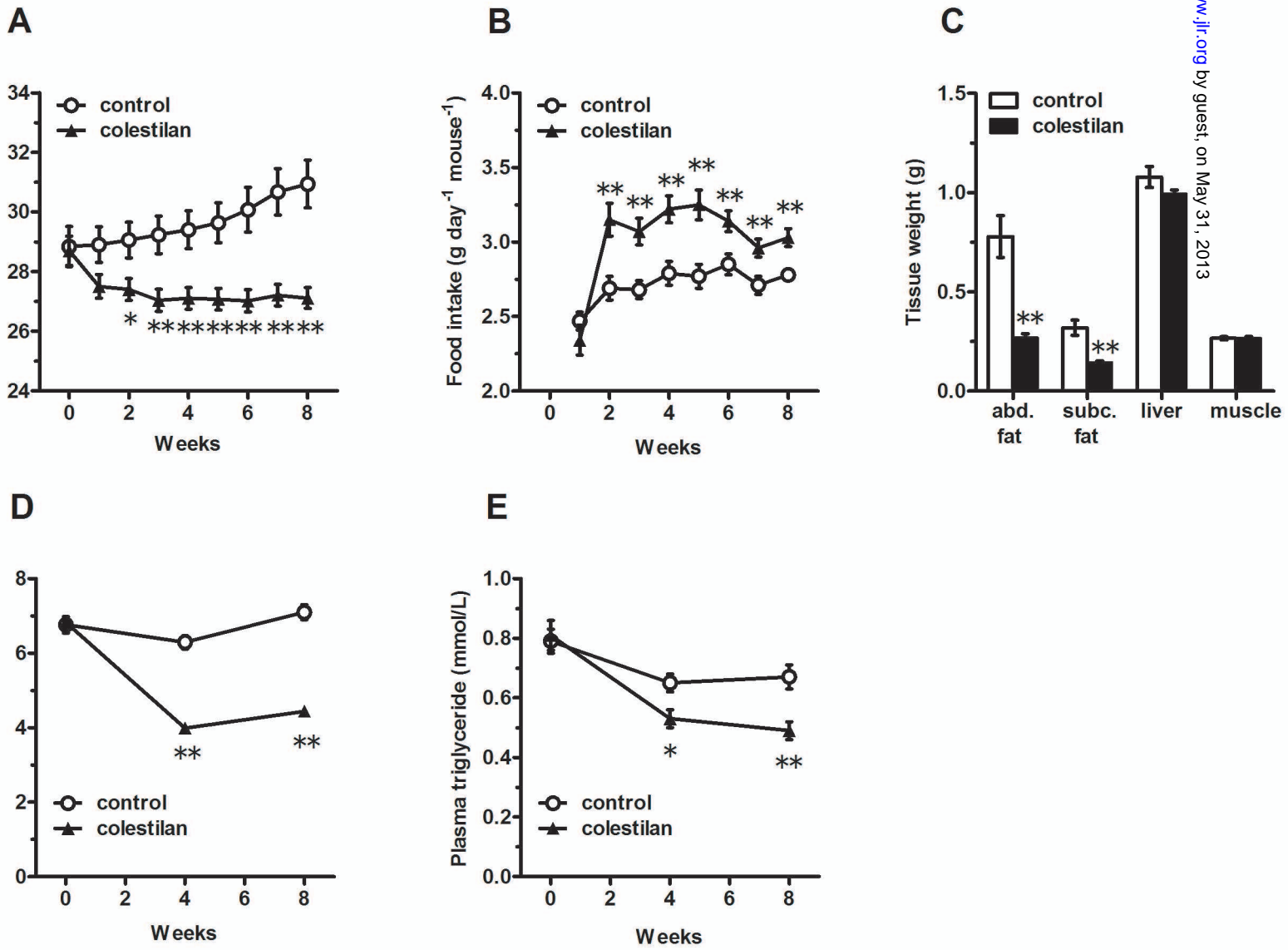
Figure 5

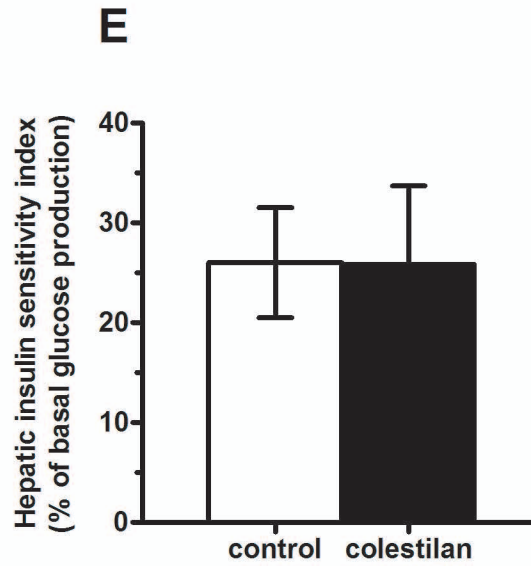
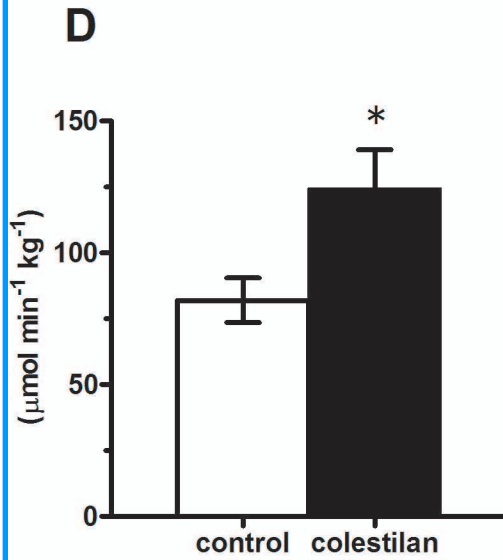
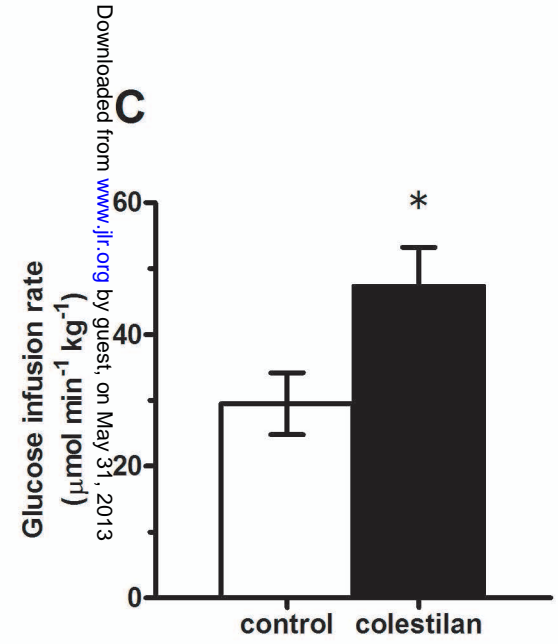
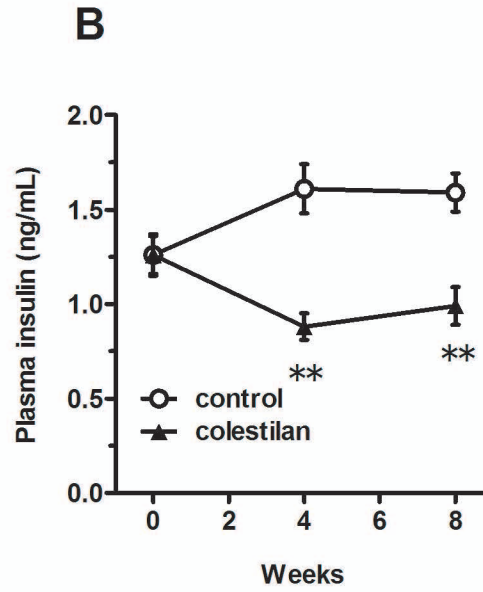
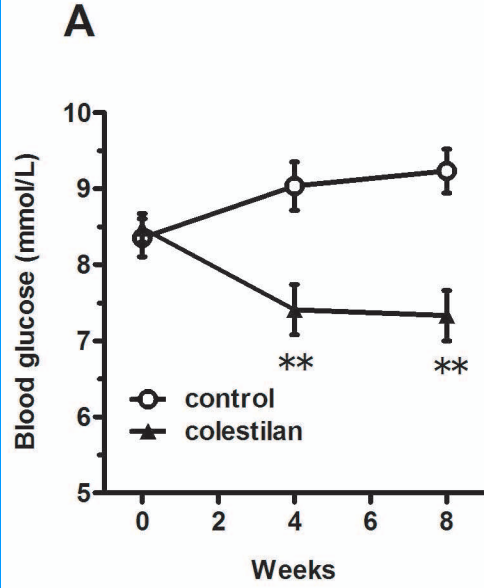
Colestilan increases [³H]-NEFA-derived radioactivity in biliary lipids and decreases plasma NEFA levels. In [³H]-NEFA infusion analysis combined with bile duct cannulation, the following parameters were determined after overnight fasting (n = 5–8): total and [³H]-bile acid in bile (A, B), total and [³H]-cholesterol in bile (C, D), total and [³H]-phospholipid in

bile (E, F), and total amount of collected bile (G). Plasma NEFA (H) was measured after 4-h fasting in high-fat-fed E3L mice (n=20–21). Data are expressed as means \pm SE. * p < 0.05, ** p < 0.01 vs. control by Student's *t*-test.

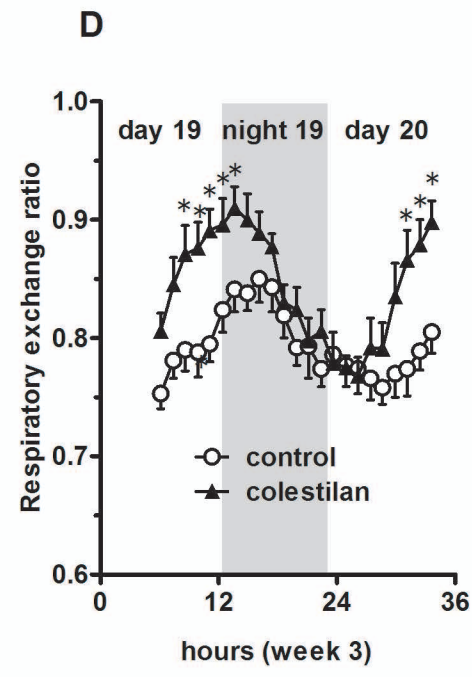
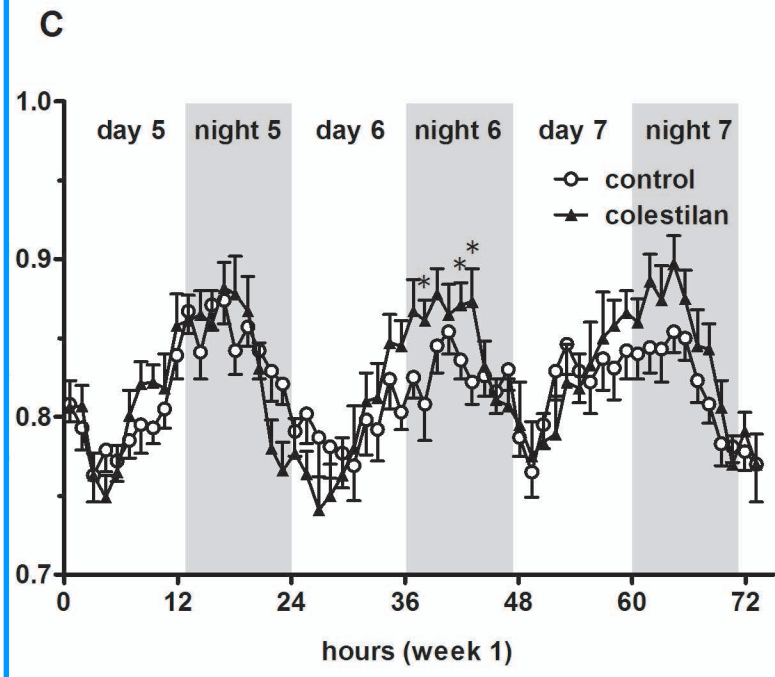
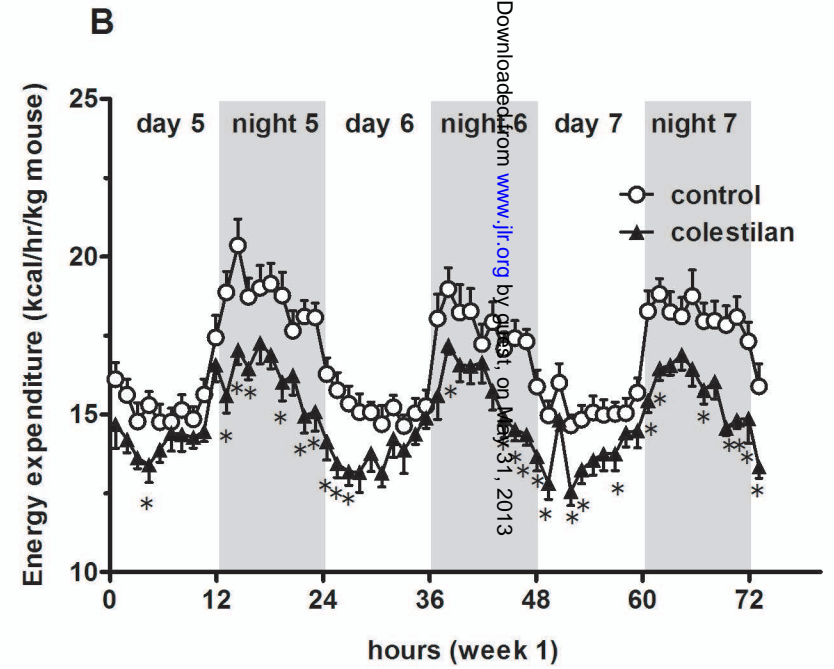
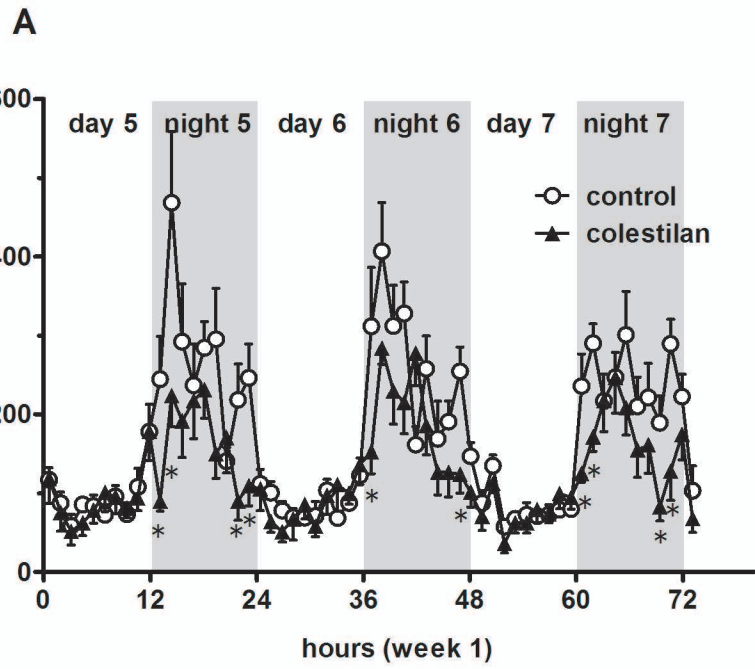
Figure 6

Effect of colestilan on gene expressions in liver, adipose tissue and muscles involved in lipid and glucose metabolism. Mice received a high fat diet or high fat diet with colestilan for 8 weeks. Livers, adipose tissues and muscles were collected after 4-h fasting, total RNA was extracted and gene expression analysis was performed using Affymetrix MOE430A arrays. Data represent fold change as compared to the control group. Values in bold are considered significant (p <0.05). Red box indicates increase, blue box decrease. Only those genes that were significantly affected by colestilan treatment in either one or more tissues are shown in this figure. For complete data, see Supplemental figure.



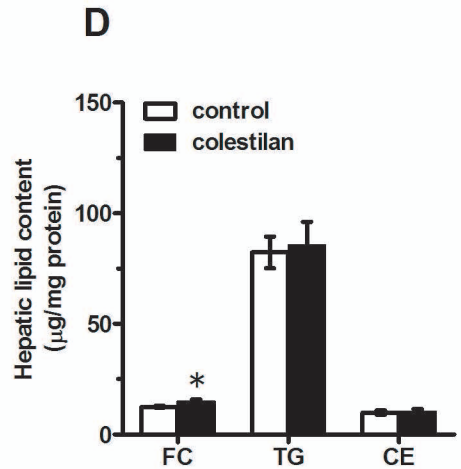
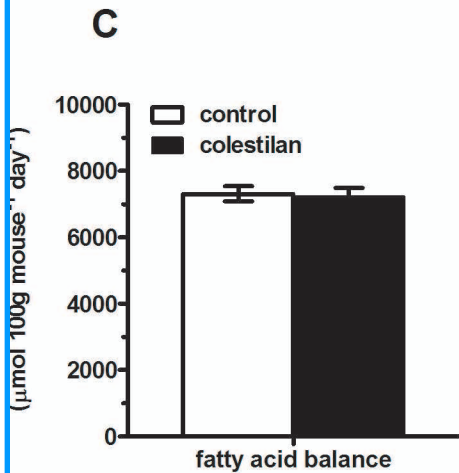
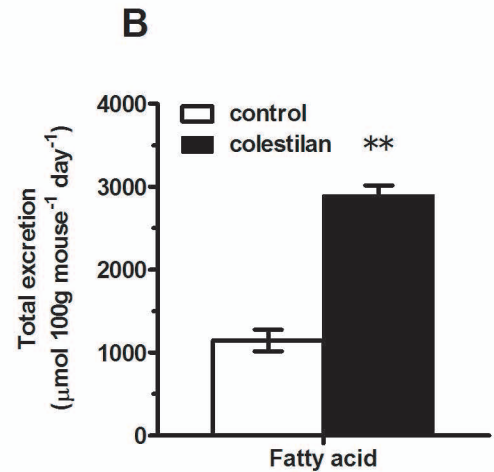
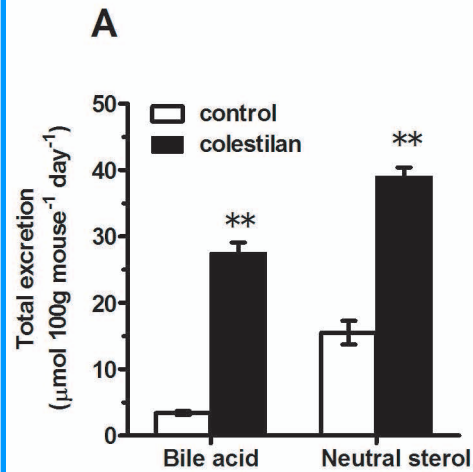


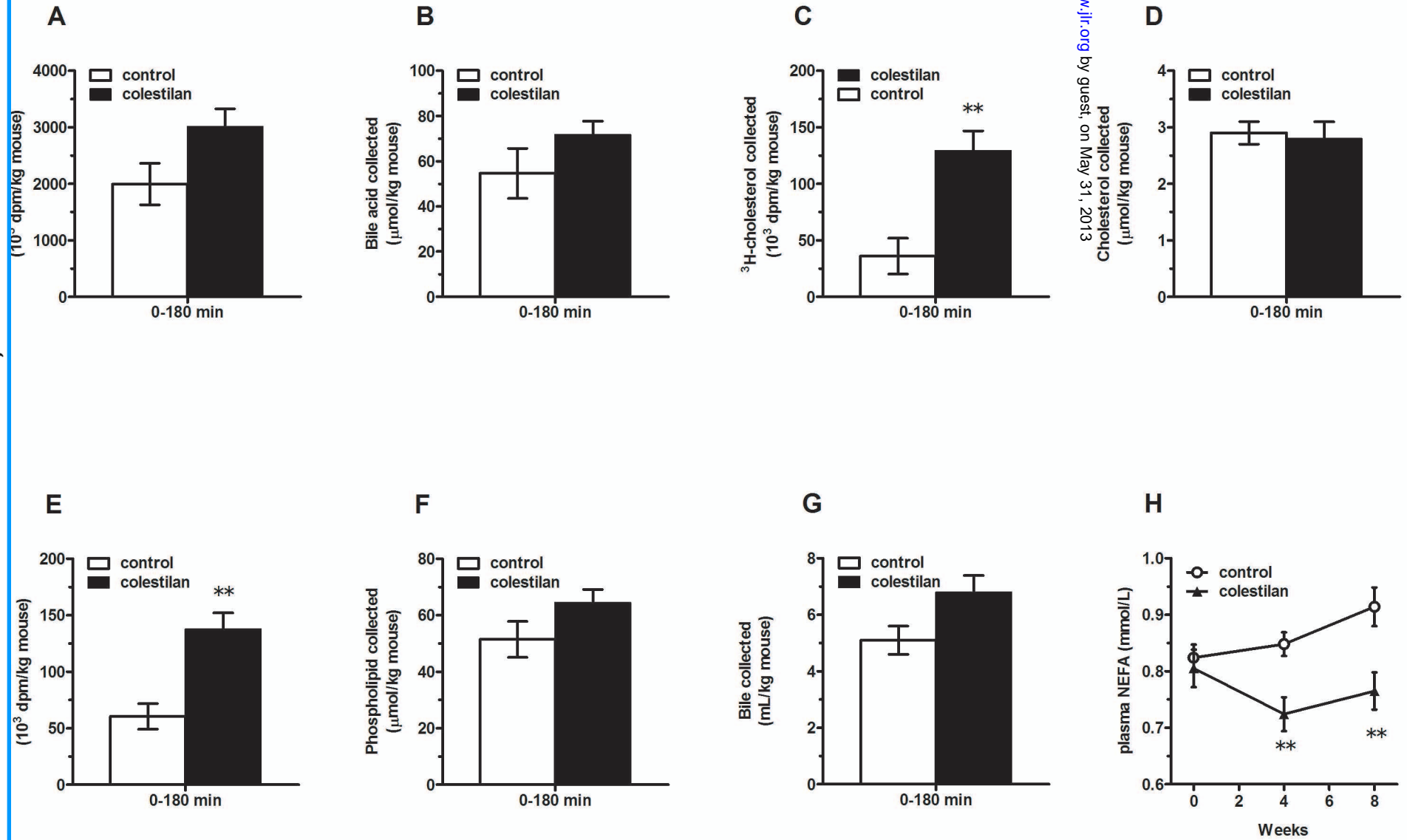
Downloaded from www.jlr.org by guest, on May 31, 2013



Downloaded from www.jlr.org by guest on May 31, 2013

Sugimoto-Kawabata et al, Figure 4





Sugimoto-Kawabata et al, Figure 6

Protein	Gene	Fold-change			Description
		Liver	Fat	Muscle	
Transcription factors					
LXRb	Nr1h2	-1.57	-1.32	-1.10	nuclear receptor subfamily 1, group H, member 2
PPARa	Ppara	6.20	1.21	-1.06	peroxisome proliferator activated receptor alpha
PPARg	Pparg	1.62	1.21	-1.26	peroxisome proliferator activated receptor gamma
CAR	Nr1h3	1.74	1.17	-1.03	nuclear receptor subfamily 1, group I, member 3
FXR	Nr1h4	1.51	1.19	1.09	nuclear receptor subfamily 1, group H, member 4
PXR	Nr1h2	2.22	1.16	1.10	nuclear receptor subfamily 1, group I, member 2
SHP	Nr0b2	-4.55	1.17	1.07	nuclear receptor subfamily 0, group B, member 2
Hnf4a	Nr2a1	1.54	1.04	-1.08	hepatic nuclear factor 4, alpha
ChREBP	Mxipl	-5.07	-1.50	1.03	MLX interacting protein-like
Lipolysis					
LPL	Lpl	-1.73	1.18	1.01	lipoprotein lipase
ApoC3	Apoc3	-1.19	1.09	-2.24	apolipoprotein C-III
FATG synthesis					
FAS	Fasn	1.05	1.09	1.57	fatty acid synthase
DGAT1	Dgat1	1.33	1.37	1.66	diacylglycerol O-acyltransferase 1
SCD	Scd1	1.24	1.17	-2.44	stearoyl-Coenzyme A desaturase 1
ACLY	Acly	1.52	-1.15	1.07	ATP citrate lyase
S14	Thrsp	1.73	-1.04	1.92	thyroid hormone responsive SPOT14 homolog (Rattus)
ACSL1	Acs1f	1.05	1.94	-1.16	acyl-CoA synthetase long-chain family member 1
ACSL5	Acs1f	1.81	-1.09	1.30	acyl-CoA synthetase long-chain family member 5
ACSS1	Acss1	1.05	-1.53	1.17	acyl-CoA synthetase short-chain family member 1
ACSS2	Acss2	2.24	-1.21	-1.29	acyl-CoA synthetase short-chain family member 2
ACSM3	Acsm3	1.20	1.66	1.02	acyl-CoA synthetase medium-chain family member 3
Beta oxidation					
Bifunctional enzyme	Ehhadh	1.18	-1.05	1.85	enoyl-Coenzyme A, hydratase/3-hydroxyacyl Coenzyme A dehydrogenase
Thiolase 1b	Acaa1b	1.07	1.39	-1.70	acetyl-Coenzyme A acyltransferase 1B
ACSL1	Acs1f	1.05	1.94	-1.16	acyl-CoA synthetase long-chain family member 1
ACSL5	Acs1f	1.81	-1.09	1.30	acyl-CoA synthetase long-chain family member 5
ACSS1	Acss1	1.05	-1.53	1.17	acyl-CoA synthetase short-chain family member 1
ACSS2	Acss2	2.24	-1.21	-1.29	acyl-CoA synthetase short-chain family member 2
ACSM3	Acsm3	1.20	1.66	1.02	acyl-CoA synthetase medium-chain family member 3
FA uptake, transport, binding					
FABP1	Fabp1	-1.14	1.75	-6.50	fatty acid binding protein 1, liver
FABP2	Fabp2	-7.56	1.24	-1.19	fatty acid binding protein 2, intestinal
FABP4	Fabp4	-1.92	1.04	-1.02	fatty acid binding protein 4, adipocyte
FABP6	Fabp6	1.06	1.52	-1.18	fatty acid binding protein 6, ileal (gastrotropin)
FATPa2	Slc27a2	1.09	1.57	-1.58	solute carrier family 27 (fatty acid transporter), member 2
FATPa4	Slc27a4	-1.22	-1.70	-1.01	solute carrier family 27 (fatty acid transporter), member 4
VLDL metabolism					
ApoBEC1	Apobec1	-1.29	-1.57	1.08	apolipoprotein B mRNA editing enzyme, catalytic polypeptide 1
Phospholipid metabolism					
PCYT1a	Pcyt1a	2.73	-1.11	-1.74	phosphate cytidylyltransferase 1, choline, alpha isoform
CDS2	Cds2	1.74	-1.16	-1.01	CDP-diacylglycerol synthase (phosphatidate cytidylyltransferase) 2
LPCAT3	Lpcat3	1.53	-1.43	-1.22	lysophosphatidylcholine acyltransferase 3
ABCB4	Abcb4	1.27	1.08	1.57	ATP-binding cassette, sub-family B (MDR/TAP), member 4
Cholesterol synthesis					
ACAT2	Acat2	2.45	-1.37	1.17	acetyl-Coenzyme A acetyltransferase 2
ACLY	Acly	1.52	-1.15	1.07	ATP citrate lyase
HMG CoA reductase	Hmgcr	7.34	-1.12	1.16	3-hydroxy-3-methylglutaryl-Coenzyme A reductase
HMG CoA synthase	Hmgcs2	-1.29	-1.34	-1.52	3-hydroxy-3-methylglutaryl-Coenzyme A synthase 2
Squalene synthase	Fdf1	2.08	-1.61	1.44	farnesyl diphosphate farnesyl transferase 1
Cholesterol excretion					
ABCA1	Abca1	-1.06	1.74	-1.05	ATP-binding cassette, sub-family A (ABC1), member 1
Bile acid synthesis					
CYP7a1	Cyp7a1	21.15	1.20	1.05	cholesterol 7 alpha hydroxylase (cyp7a1)
Gluconeogenesis					
SLC37A4	Slc37a4	1.54	-1.25	-1.01	glucose-6-phosphatase transport protein 1 (g6pt1)
Glycolysis					
GLUT4	Slc2a4	1.32	1.54	-1.51	facilitated glucose transport member 4 (glut4)
PK3	Pkm	-2.40	-1.09	-1.03	pyruvate kinase 3 (pk3)
Insulin regulation					
IRS1	Irs1	-1.50	-1.08	-1.74	insulin receptor substrate 1 (irs1)
Leptin	Lep	1.05	-1.42	-2.18	leptin (lep)
Thermal regulation					
UCP1	Ucp1	1.04	-1.01	8.97	uncoupling protein 1 (ucp1)
UCP2	Ucp2	-1.73	-2.31	1.12	uncoupling protein 2 (ucp2)